Research Article
Vortices in Vacuumless Systems

M. A. Marques

Departamento de Física, Universidade Federal da Paraíba, 58051-970 João Pessoa, PB, Brazil

Correspondence should be addressed to M. A. Marques; mam.matheus@gmail.com

We investigate the presence of vortex solutions in potentials without vacuum state. The study is conducted considering Maxwell and Chern-Simons dynamics. Also, we use a first-order formalism that helps us to find the solutions and their respective electromagnetic fields and energy densities. As a bonus, we get to calculate the energy without knowing the explicit solutions. Even though the solutions present a large "tail" which goes far away from the origin, the magnetic flux remains a well defined topological invariant.

1. Introduction

In high energy physics, topological structures appear in a diversity of contexts and have been vastly studied over the years [1, 2]. In spatial dimensions lower than three, the most known ones are kinks and vortices, which are static solutions of the equations of motion.

The simplest structures are kinks, which appear in $(1, 1)$ spacetime dimensions by the action of scalar fields [3]. Kinks connect the minima of the potential and have a topological character that ensures its stability. However, it was shown in [4] that topological defects may arise in potentials without a vacuum state, whose minima are located at infinity. Regarding the kink in the vacuumless system, it is asymptotically divergent and has infinite amplitude. Nevertheless, it is stable and can be associated with a topological charge by using a special definition for the topological current [5]. Over the years, many papers have studied vacuumless topological defects in a diversity of contexts in high energy physics [6–14].

Potentials with extrema at infinity, similar to the ones we are going to study here, although inverted, also appear in classical mechanics [15]. In this scenario, if the energy is small enough, the motion is bounded. As the energy gets higher, the boundary values become far form each other, until the limit where they are infinitely separated. This limit distinguishes bounded and unbounded motion, so for sufficiently high values of the energy, the motion becomes unbounded. A similar situation happens in the interaction of a body with the gravitational potential, $V \propto -1/r$, which vanishes only at $r \longrightarrow \infty$, when one calculates the escape velocity: the zero energy of the system describes the limit between bounded and unbounded motion. In high energy physics, vacuumless potentials arise in the massless limit of supersymmetric QCD due to nonperturbative effects [16]. They also appear in the cosmological context, where their energy densities could act as a cosmological constant that decreases slower than the densities of matter and radiation [17, 18].

By working in $(2, 1)$ spacetime dimensions one can find vortices. The first relativistic model that supports these objetcs was studied in [19, 20], with the action of a complex scalar field coupled to a gauge field under the symmetry $U(1)$ in Maxwell dynamics. These structures are electrically neutral and engender a quantized flux which is conserved and works as a topological invariant. Their equations of motion are of second order with couplings between the fields; thus, they are hard to be solved. To simplify the problem, the BPS formalism was developed in [21, 22] for this model, which allowed for the presence of first order equations and the energy without knowing the explicit form of the solutions.

Models with the gauge field governed by the Maxwell dynamics, however, are not the only ones which support vortices solutions. One can also investigate these structures with the dynamics of the gauge field governed by the Chern-Simons term [23–25]. In this case, the vortex presents a quantized flux, which also is topological invariant, and a

quantized electric charge. The first studies of vortices in Chern-Simons dynamics are [26–28]; for more on this, see [29].

The importance of vortices in high energy physics and in other areas of physics can be found in [1, 2, 30]. For instance, they may appear during the cosmic evolution of our Universe [1] and in models that includes the so-called hidden sector, which is of interest in dark matter [31–34], by enlarging the symmetry to $U(1) \times U(1)$; see [35–37]. Following this direction of enlarged symmetries, they are also present in $U(1) \times SO(3)$ models, with the addition of extra degrees of freedom to the vortex via the inclusion of a triplet scalar field, and in $U(1) \times Z_2$ models, with the inclusion of a neutral scalar field that acts as a source to the internal structure of the vortex [38]. Other motivations come from the context of condensed matter, where they may emerge in superconductors and in magnetic materials as magnetic domains [39]. They may also appear in dipolar Bose-Einstein condensates, where the atoms interact as dipole-dipole, which leads to the presence of non standard vortex structures [40–42].

Topological structures may be studied with generalized models [43, 44]. Vortices, in particular, firstly appeared in noncanonical models in [45, 46]. Since then, several works arised with other motivations. In the context of inflation, for instance, a model with a modified kinetic term was introduced in [47]. In this scenario, these models present distinct features from the standard case: they may not need a potential to drive the inflation. Moreover, generalized models were used in [48, 49] as a tentative to explain why the universe is accelerated at a late stage of its evolution.

Noncanonical models considering defect structures were severely investigated over the years [50–63]. Among the many investigations, a first-order formalism was developed for some classes of noncanonical models in [45, 46, 60, 64, 65]. However, only in [66] it was completely developed for any generalized model. An interesting fact is that compact structures, which were firstly presented in [67], are possible to appear as Maxwell and Chern-Simons vortices only if generalized models are considered; see [68, 69]. Noncanonical models also allow for the presence of vortices that share the same field configuration and energy density, known as twinlike models [70].

This work deals with a class of generalized Maxwell and Chern-Simons models that support vortex solutions in vacuumless systems. In Section 2, we investigate the properties of vortices with Maxwell dynamics, including its first-order formalism, and introduce two new models, one of them with analytical results. In Section 3 we conduct a similar investigation, however in the Chern-Simons scenario, also considering its first-order formalism, and we introduce two new models. Finally, in Section 4 we present our ending comments and conclusions.

2. Maxwell-Higgs Models

We deal with an action in $(2, 1)$ flat spacetime dimensions for a complex scalar field and a gauge field governed by the Maxwell dynamics. We follow the lines of [66] and write $S = \int d^3 x \mathscr{L}$, with the Lagrangian density given by

$$\mathscr{L} = -\frac{1}{4} F_{\mu\nu} F^{\mu\nu} + K(|\varphi|) \overline{D_\mu \varphi} D^\mu \varphi - V(|\varphi|). \tag{1}$$

In the above equation, φ denotes the complex scalar field, A^μ is the gauge field, $F_{\mu\nu} = \partial_\mu A_\nu - \partial_\nu A_\mu$ represents the electromagnetic strength tensor, $D_\mu = \partial_\mu + ieA_\mu$ stands for the covariant derivative, e is the electric charge, and $V(|\varphi|)$ is the potential, which is supposed to present symmetry breaking. The function $K(|\varphi|)$ is dimensionless and, in principle, arbitrary. Nevertheless, it has to admit solutions with finite energy. It is straightforward to show that $K(|\varphi|) = 1$ gives the standard case considered in [19]. One may vary the action with respect to the fields φ and A_μ to get the equations of motion

$$D_\mu (K D^\mu \varphi) = \frac{\varphi}{2|\varphi|} \left(K_{|\varphi|} \overline{D_\mu \varphi} D^\mu \varphi - V_{|\varphi|} \right), \tag{2a}$$

$$\partial_\mu F^{\mu\nu} = J^\nu, \tag{2b}$$

where the current is $J_\mu = ieK(|\varphi|)(\overline{\varphi} D_\mu \varphi - \varphi \overline{D_\mu \varphi})$ and $V_{|\varphi|} = dV/d|\varphi|$. Invariance under spacetime translations, $x^\mu \longrightarrow x^\mu + a^\mu$, with a^μ constant, leads to the energy momentum tensor

$$T_{\mu\nu} = F_{\mu\lambda} F^\lambda_\nu + K(|\varphi|) \left(\overline{D_\mu \varphi} D_\nu \varphi + \overline{D_\nu \varphi} D_\mu \varphi \right) - \eta_{\mu\nu} \mathscr{L}. \tag{3}$$

In order to investigate vortex solutions in the model, we consider static configurations. As a consequence, the $\nu = 0$ component of (2b) becomes an identity under the choice $A_0 = 0$. This makes the electric field vanish, so the vortex is electrically uncharged. Since we are dealing with two spatial dimensions, we define the magnetic field as $B = -F^{12}$. In this case, the surviving components of the energy momentum tensor (3) are

$$T_{00} = \frac{B^2}{2} + K(|\varphi|) |D_i \varphi|^2 + V(|\varphi|), \tag{4a}$$

$$T_{12} = K(|\varphi|) \left(\overline{D_1 \varphi} D_2 \varphi + \overline{D_2 \varphi} D_1 \varphi \right), \tag{4b}$$

$$T_{11} = \frac{B^2}{2} + K(|\varphi|) \left(2 |D_1 \varphi|^2 - |D_i \varphi|^2 \right) - V(|\varphi|), \tag{4c}$$

$$T_{22} = \frac{B^2}{2} + K(|\varphi|) \left(2 |D_2 \varphi|^2 - |D_i \varphi|^2 \right) - V(|\varphi|). \tag{4d}$$

The energy density is $\rho = T_{00}$ and the components T_{ij} define the stress tensor. We then take the usual ansatz for vortex solutions

$$\varphi(r, \theta) = g(r) e^{in\theta}, \tag{5a}$$

$$A_i = -\epsilon_{ij} \frac{x^j}{er^2} [a(r) - n], \tag{5b}$$

where r and θ are the polar coordinates and $n = \pm 1, \pm 2, \ldots$ is the vorticity. The functions $g(r)$ and $a(r)$ must obey the boundary conditions

$$g(0) = 0,$$
$$a(0) = n,$$
$$\lim_{r \to \infty} g(r) = v, \qquad (6)$$
$$\lim_{r \to \infty} a(r) = 0.$$

In the above equations, v is a parameter that is involved in the symmetry breaking of the potential. Considering the ansatz (5a) and (5b), the magnetic field becomes

$$B(r) = -\frac{a'}{er}. \qquad (7)$$

By integrating it all over the space one can show that the flux is given by

$$\Phi = \int d^2x\, B$$
$$= \frac{2\pi n}{e}. \qquad (8)$$

Therefore, the magnetic flux is conserved and quantized by the vorticity n. As one knows, it is possible to introduce the conserved topological current

$$j_T^\mu = \epsilon^{\mu\nu\lambda}\partial_\lambda A_\nu, \qquad (9)$$

in which the component $j_T^0 = B$ plays the role of a topological charge density. By integrating this, one can see that the flux (8) plays an important role in the theory since it gives the topological charge of the system.

The equations of motion (2a) and (2b) with the ansatz (5a) and (5b) become

$$\frac{1}{r}\left(rKg'\right)' = \frac{Ka^2 g}{r^2} + \frac{1}{2}V_g, \qquad (10a)$$

$$r\left(\frac{a'}{r}\right)' = 2e^2 K a g^2. \qquad (10b)$$

Moreover, the components of the energy momentum tensor with the ansatz take the form

$$T_{00} = \frac{a'^2}{2e^2 r^2} + K(g)\left(g'^2 + \frac{a^2 g^2}{r^2}\right) + V(g), \qquad (11a)$$

$$T_{12} = K(g)\left(g'^2 - \frac{a^2 g^2}{r^2}\right)\sin(2\theta), \qquad (11b)$$

$$T_{11} = \frac{a'^2}{2e^2 r^2} + K(g)$$
$$\cdot \left(g'^2\left(2\cos^2\theta - 1\right) + \frac{a^2 g^2}{r^2}\left(2\sin^2\theta - 1\right)\right) \qquad (11c)$$
$$- V(g),$$

$$T_{22} = \frac{a'^2}{2e^2 r^2} + K(g)$$
$$\cdot \left(g'^2\left(2\sin^2\theta - 1\right) + \frac{a^2 g^2}{r^2}\left(2\cos^2\theta - 1\right)\right) \qquad (11d)$$
$$- V(g).$$

As was shown in [66], the stability against contractions and dilatations in the solutions requires the stressless condition. By setting $T_{ij} = 0$, we get the first-order equations

$$g' = \pm\frac{ag}{r}$$
$$\text{and} \quad -\frac{a'}{er} = \pm\sqrt{2V(g)}. \qquad (12)$$

The pair of equations for the upper signs are related to the lower signs ones by the change $a(r) \longrightarrow -a(r)$. These equations are compatible with the equations of motion (10a) and (10b) if the potential and the function $K(|\varphi|)$ are constrained by

$$\frac{d}{dg}\sqrt{2V(g)} = -2egK(g). \qquad (13)$$

For $K(g) = 1$, we have $V(|\varphi|) = e^2(v^2 - |\varphi|^2)^2/2$, which is the standard case firstly studied in [19]. This constraint shows that generalized models are required to study different potentials and their correspondent vortexlike solutions from the ones of the standard case. The first-order equations (12) also gives rise to the possibility of introducing an auxiliary function $W(a, g)$ in the form

$$W(a, g) = -\frac{a}{e}\sqrt{2V(g)}, \qquad (14)$$

so the energy density is written as

$$\rho = \frac{1}{r}\frac{dW}{dr}. \qquad (15)$$

By integrating it all over the space, we get the energy

$$E = 2\pi\left|W(a(\infty), g(\infty)) - W(a(0), g(0))\right|$$
$$= 2\pi\left|W(0, v) - W(n, 0)\right|. \qquad (16)$$

Thus, the energy of the stressless solutions may be calculated without knowing their explicit form. Below, by properly choosing $K(|\varphi|)$ and $V(|\varphi|)$ that satisfy the constraint in (13), we show new models that engender a set of minima of the potential at infinity. Thus, we have $v = \infty$ in (6). In order to prepare the model for numerical investigation, we work with dimensionless fields and consider unit vorticity, $n = 1$, which requires the upper signs in the first-order equations (12).
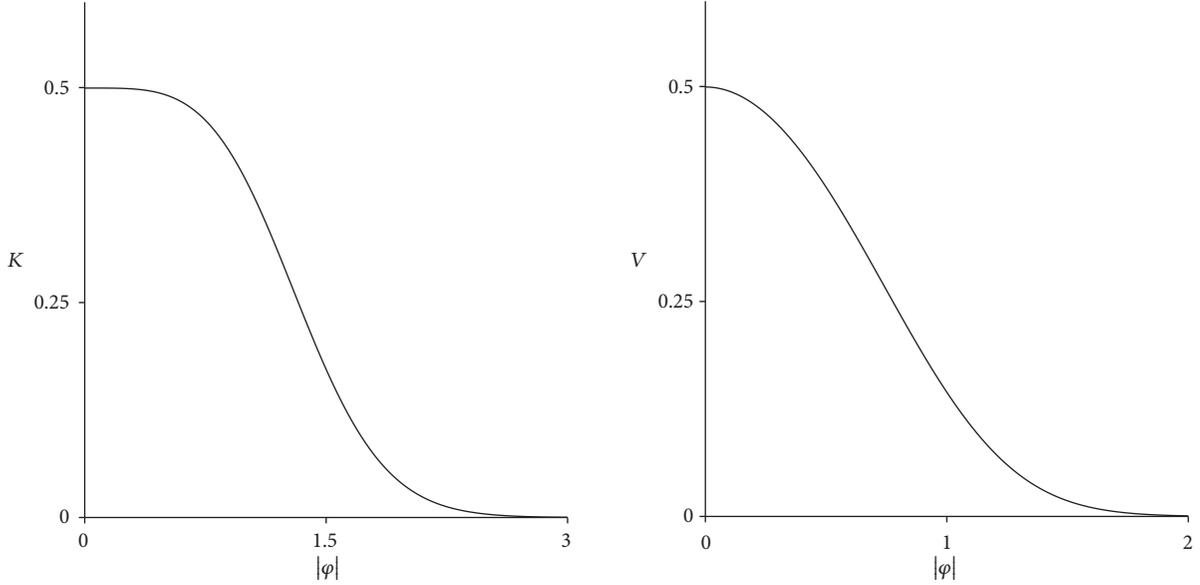
FIGURE 1: The function $K(|\varphi|)$ (left) and the potential $V(|\varphi|)$ (right) given by (17a) and (17b).

2.1. First Model. The first example is given by the pair of functions

$$K\left(|\varphi|\right) = \frac{1}{2}\text{sech}^2\left(\frac{1}{2}|\varphi|^2\right), \tag{17a}$$

$$V\left(|\varphi|\right) = \frac{1}{2}\left(1 - \tanh\left(\frac{1}{2}|\varphi|^2\right)\right)^2. \tag{17b}$$

The above potential does not present a vacuum state; that is the reason we call it vacuumless potential. However, since $V(\infty) = 0$, we see the set of mimima of the potencial is located at infinity, which allows it to support vortex solutions. Its maximum is at $|\varphi_m| = 0$, with $V(|\varphi_m|) = 1/2$. In Figure 1 we plot the above functions. We see that $K(|\varphi|)$, which is the function that controls the kinetic term of the model, behaves similarly to the potential $V(|\varphi|)$, having a maximum in the origin and its set of minima at infinity.

For this model, the first-order equations (12) become

$$g' = \frac{ag}{r}$$

$$\text{and } \frac{a'}{r} = -\left(1 - \tanh\left(\frac{g^2}{2}\right)\right). \tag{18}$$

Near the origin, we can study the behavior of the solutions by taking $a(r) = 1 - a_0(r)$ and $g(r) = g_0(r)$ and going up to first order in $a_0(r)$ and $g_0(r)$. By substituting them in the above equations, we get that

$$a_0(r) \propto r^2$$

$$\text{and } g_0(r) \propto r. \tag{19}$$

It is worth commenting that, in this case, since the set of minima of the potential are at infinity, we see from the boundary conditions (6) that $g(r)$ is asymptotically divergent

and has infinite amplitude; i.e., $g(r \longrightarrow \infty) \longrightarrow \infty$. Nevertheless, even though $g(r)$ goes to infinity, $a(r)$ still vanishes at infinity, similarly to what happens in the standard case.

Although (18) are of first order, their nonlinearities make the job of finding analytical solutions very hard. Unfortunately, we have not been able to find them for these equations. Therefore, we must solve them by using numerical methods. In Figure 2, we plot the solutions of the above equations. Near the origin, we see that the functions vary as expected from (19). As r increases, they tend to their boundary values very slow, which makes the tail of the solutions be present far away from the origin. This behavior is exactly the opposite from the one that appears in models which support compact vortices, in which the solutions attain their boundary values at a finite r [68].

Before going further, we calculate the function $W(a, g)$, given by (14):

$$W\left(a, g\right) = -a + a\tanh\left(\frac{g^2}{2}\right). \tag{20}$$

By using (16), it is straightforward to show that the solutions of (18) have energy $E = 2\pi$. The magnetic field is given by (7) and the energy density can be calculated from (11a), which becomes

$$\rho\left(r\right) = \frac{a'^2}{2e^2 r^2} + \frac{1}{2}\text{sech}^2\left(\frac{g^2}{2}\right)\left(g'^2 + \frac{a^2 g^2}{r^2}\right)$$

$$+ \frac{1}{2}\left(1 - \tanh\left(\frac{g^2}{2}\right)\right)^2. \tag{21}$$

We then use our numerical solutions and plot the magnetic field and the energy density in Figure 3. One can see the large tail that the solutions have far away from the origin is less
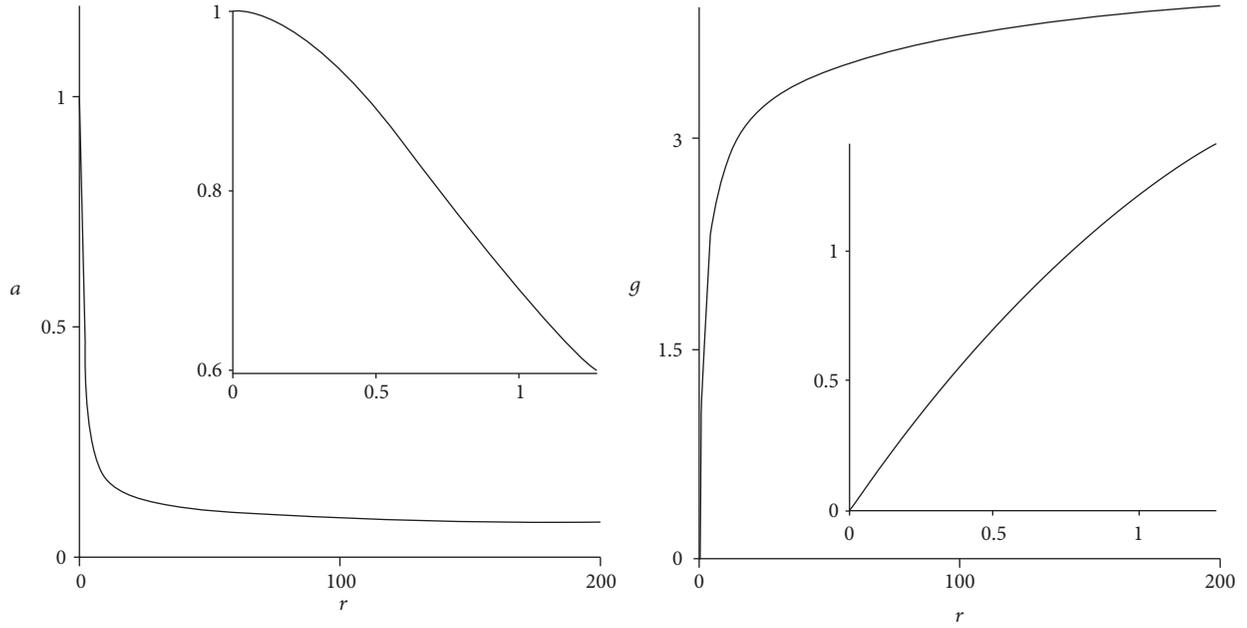
FIGURE 2: The solutions $a(r)$ (left) and $g(r)$ (right) of (18). The insets show the behavior of the functions near the origin, in the interval $r \in [0, 1.27]$.
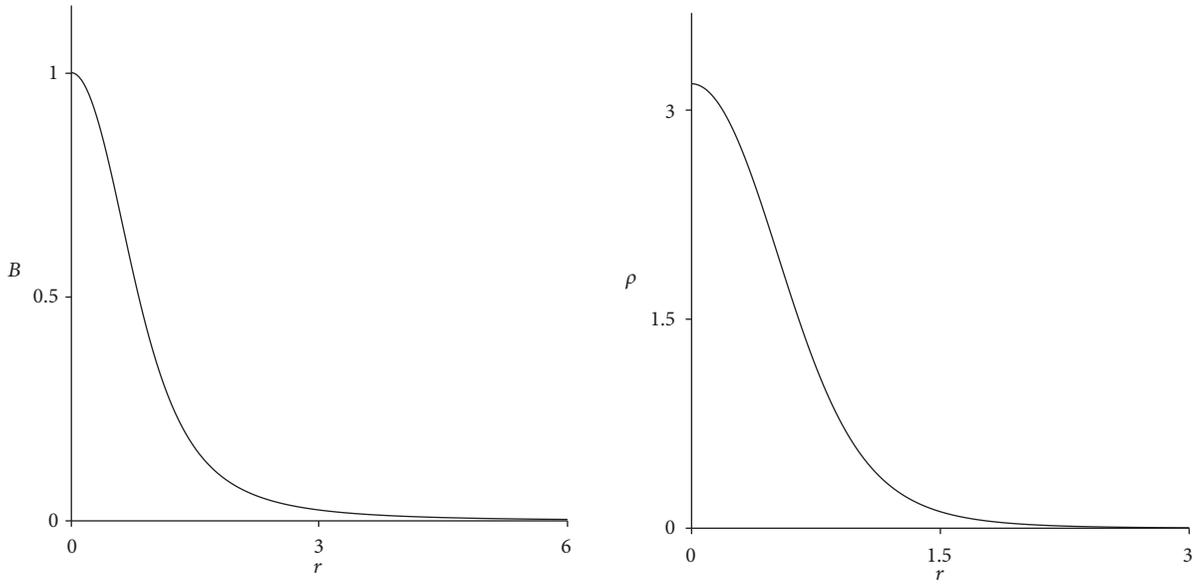

FIGURE 3: The magnetic field (left) and the energy density (right) for the solutions of (18).

evident in the magnetic field and in the energy density. By numerical integration, one can show that the magnetic flux is well defined and given by $\Phi \approx 2\pi$, as expected from (8). Since the flux gives the topological charge associated with the vortex, this well defined behavior is different from the one for kinks in vacuumless systems, which require a special definition of topological current to get a topological character well defined [5]. The numerical integration of the energy density all over the space gives energy $E \approx 2\pi$, which matches the value obtained with the using of the function $W(a, g)$ in (20).

2.2. Second Model.

Our second model arises from the pair of functions

$$K\left(|\varphi|\right) = \frac{\left(2 - \left(4 - 3S^2\right)C^2\right)S^2 + \left(2 - 3S^2\right)SC}{2\left|\varphi\right|^4}, \quad (22a)$$

$$V\left(|\varphi|\right) = \frac{(1 - SC)^2 S^4}{2\left|\varphi\right|^4}, \quad (22b)$$

in which we have used the notation $S = \operatorname{sech}(|\varphi|)$ and $C = |\varphi| \operatorname{csch}(|\varphi|)$. Given the above expressions, one may
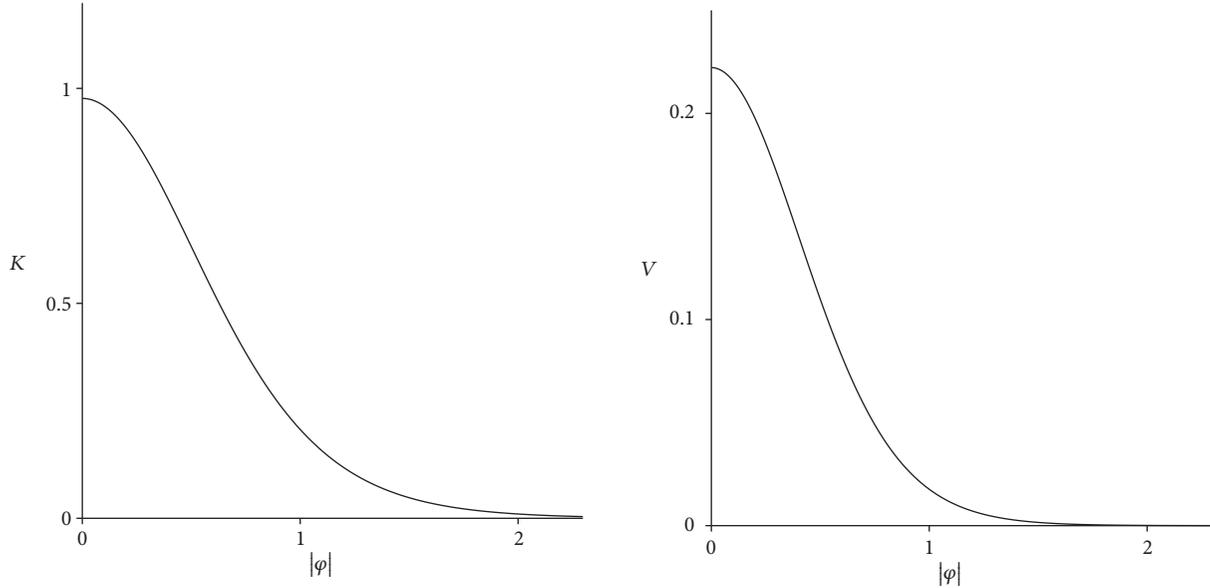
FIGURE 4: The function $K(|\varphi|)$ (left) and the potential $V(|\varphi|)$ (right) given by (22a) and (22b).

wonder if these functions are finite in the origin. It is worth to investigate their behavior for $|\varphi| \approx 0$, which is given by

$$K_{|\varphi|\approx 0}(|\varphi|) = \frac{44}{45} - \frac{1676}{945}|\varphi|^2 + \mathcal{O}\left(|\varphi^4|\right), \tag{23a}$$

$$V_{|\varphi|\approx 0}(|\varphi|) = \frac{2}{9} - \frac{88}{135}|\varphi|^2 + \mathcal{O}\left(|\varphi^4|\right). \tag{23b}$$

Then, they are regular at $|\varphi_m| = 0$, which is a point of maximum with $V(|\varphi_m|) = 2/9$. As in the previous model, this potential also is vacuumless. In Figure 4, we plot these functions. Notice that $K(|\varphi|)$ behaves similarly to the potential.

In this case, the first-order equations (12) take the form

$$g' = \frac{ag}{r}, \tag{24a}$$

$$\frac{a'}{r} = -\frac{\left(1 - g \operatorname{sech}(g) \operatorname{csch}(g)\right) \operatorname{sech}^2(g)}{g^2}. \tag{24b}$$

The behavior near the origin can be studied by considering $a(r) = 1 - a_0(r)$ and $g(r) = g_0(r)$ and going up to first order in $a_0(r)$ and $g_0(r)$. Plugging them in the above equations, we get the same behavior of (19). The above equations admit the solutions

$$g(r) = \operatorname{arcsinh}(r), \tag{25a}$$

$$a(r) = \frac{r}{\sqrt{1 + r^2} \operatorname{arcsinh}(r)}. \tag{25b}$$

Therefore, as expected, $g(r)$ goes to infinity and $a(r)$ vanishes very slowly as r increases. Then, as in the previous model, the tail of the solutions is present even for large distances from the origin. This behavior is shown in Figure 5, in which we plot these solutions.

In this case, $W(a, g)$, given by (14), takes the form

$$W(a, g) = -\frac{a\left(1 - g \operatorname{sech}(g) \operatorname{csch}(g)\right) \operatorname{sech}^2(g)}{g^2}. \tag{26}$$

Then, from (16), the solutions (25a) and (25b) have energy $E = 4\pi/3$. Since we have the analytical solutions in this case, we can calculate the magnetic field from (7) and the energy density from (11a) to get

$$B(r) = \frac{r\sqrt{1 + r^2} - \operatorname{arcsinh}(r)}{r \operatorname{arcsinh}^2(r)\left(1 + r^2\right)^{3/2}}, \tag{27a}$$

$$\rho(r)$$

$$= \frac{\left(2r^2 - 3\right)\sqrt{1 + r^2} \operatorname{arcsinh}(r) - 4r \operatorname{arcsinh}^2(r)}{r \operatorname{arcsinh}^4(r)\left(1 + r^2\right)^3} \tag{27b}$$

$$+ \frac{3r\left(r^2 + 1\right)}{r \operatorname{arcsinh}^4(r)\left(1 + r^2\right)^3}.$$

In Figure 6, we plot the magnetic field and the energy density. A direct integration of the magnetic field (27a) gives exactly the flux in (8). The energy obtained by an integration of the energy density (27b) gives the same value obtained by the use of the auxiliary function $W(a, g)$ in (26); that is, $E = 4\pi/3$. As in the previous model, the long tail of the solutions does not seem to modify the flux of the vortex, which remains as in (8). Then, the topological current (9) is a definition that leads to a well behaved topological charge.

3. Chern-Simons-Higgs Models

In order to investigate the presence of vortices with the Chern-Simons dynamics, we consider the action $S = \int d^3x \mathcal{L}$
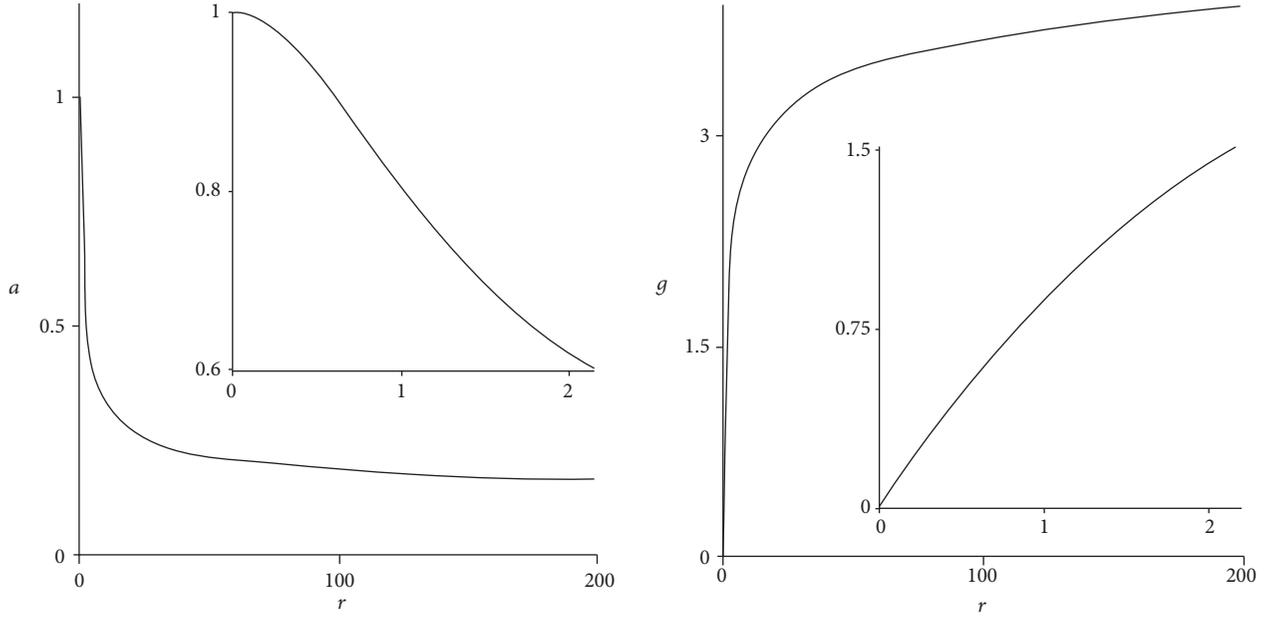
FIGURE 5: The solutions $a(r)$ (left) and $g(r)$ (right) as in (25a) and (25b). The insets show the behavior of the functions near the origin, in the interval $r \in [0, 2.16]$.
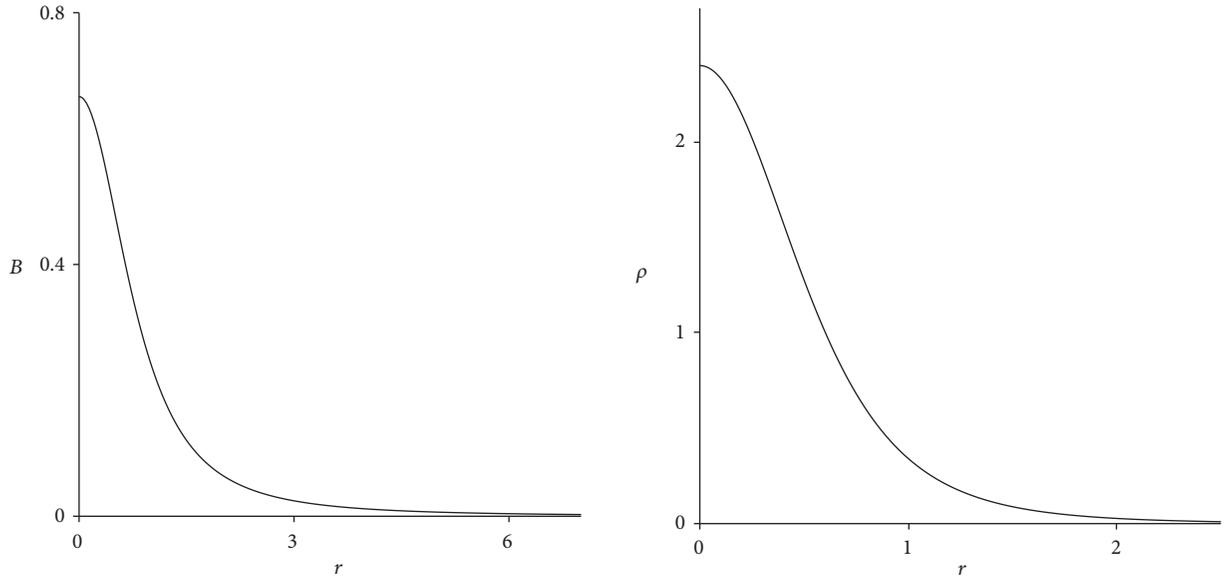

FIGURE 6: The magnetic field in (27a) (left) and the energy density as in (27b) (right).

for a complex scalar field and a gauge field. Here, we study the class of generalized models presented in [64]

$$\mathscr{L} = \frac{\kappa}{4} \epsilon^{\alpha\beta\gamma} A_\alpha F_{\beta\gamma} + K(|\varphi|) \overline{D_\mu \varphi} D^\mu \varphi - V(|\varphi|). \quad (28)$$

In the above expression, φ, A^μ, e, $D_\mu = \partial_\mu + ieA_\mu$, $F_{\mu\nu} = \partial_\mu A_\nu - \partial_\nu A_\mu$ and $V(|\varphi|)$ have the same meaning of the previous section. Here, κ is a constant. Regarding the dimensionless function $K(|\varphi|)$, it is in principle arbitrary. The only restriction for it is to provide solutions with finite energy. The standard case is given by $K(|\varphi|) = 1$ and was

studied in [27]. Here, we consider $A^\mu = (A^0, \overrightarrow{A})$. Thus, the electric and magnetic fields are

$$E^i = F^{i0} = -\dot{A}^i - \partial_i A^0$$

$$\text{and } B = -F^{12}, \quad (29)$$

with the dot meaning the temporal derivative and $(E_x, E_y) \equiv E^i$, where $i = 1, 2$. The equations of motion for the scalar and gauge fields read

$$D_\mu (KD^\mu \varphi) = \frac{\varphi}{2|\varphi|} \left(K_{|\varphi|} \overline{D_\mu \varphi} D^\mu \varphi - V_{|\varphi|} \right), \quad (30a)$$

$$\frac{\kappa}{2}\epsilon^{\lambda\mu\nu}F_{\mu\nu} = J^{\lambda}, \tag{30b}$$

where the current is $J_{\mu} = ieK(|\varphi|)(\overline{\varphi}D_{\mu}\varphi - \varphi\overline{D_{\mu}\varphi})$. Since the Chern-Simons term in the Lagrangian density (28) is metric-free, it does not contribute to the energy momentum tensor, which has the form

$$T_{\mu\nu} = K(|\varphi|)\left(\overline{D_{\mu}\varphi}D_{\nu}\varphi + \overline{D_{\nu}\varphi}D_{\mu}\varphi\right) - \eta_{\mu\nu}\left(K(|\varphi|)\overline{D_{\lambda}\varphi}D^{\lambda}\varphi - V(|\varphi|)\right). \tag{31}$$

We now consider static solutions and the same ansatz of (5a) and (5b) with the boundary conditions (6). This makes the electric and magnetic fields in (29) have the form

$$E^{i} = -\partial_{i}A_{0}$$
$$\text{and } B = -\frac{a'}{er}. \tag{32}$$

The magnetic flux can by calculated and it is given by (8), which shows that it is quantized and conserved. Therefore, the Maxwell and Chern-Simons vortices share the same magnetic flux. Furthermore, we can also consider the topological current as in (9) to show that the topological charge is given by the magnetic flux. We must be careful, though, with the temporal component of the gauge field, A_{0}. In this case, the Gauss' law that appears in (30b) for $\lambda = 0$ is not solved for $A_{0} = 0$. Moreover, A_{0} is not an independent function; one can show that it is given by

$$A_{0} = \frac{\kappa}{2e^{2}}\frac{B}{|\varphi|^{2}K(|\varphi|)}. \tag{33}$$

Since the electric field does not vanish, Chern-Simons vortices engender electric charge, given by

$$Q = \int d^{2}x J^{0}$$
$$= -\kappa\Phi. \tag{34}$$

Therefore, given the quantized magnetic flux (8), the electric charge is also quantized by the vorticity n. The equations of motion (30a) and (30b) with the ansatz (5a) and (5b) and $A_{0} = A_{0}(r)$ are given by

$$\frac{1}{r}\left(rKg'\right)' + Kg\left(e^{2}A_{0}^{2} - \frac{a^{2}}{r^{2}}\right)$$
$$+ \frac{1}{2}\left(\left(e^{2}g^{2}A_{0}^{2} - g'^{2} - \frac{a^{2}g^{2}}{r^{2}}\right)K_{g} - V_{g}\right) = 0, \tag{35a}$$

$$\frac{a'}{r} + \frac{2Ke^{3}g^{2}A_{0}}{\kappa} = 0, \tag{35b}$$

$$A_{0}' + \frac{2Keag^{2}}{\kappa r} = 0. \tag{35c}$$

The components of the energy momentum tensor (31) with the ansatz (5a) and (5b) read

$$T_{00} = \frac{\kappa^{2}}{4e^{4}}\frac{a'^{2}}{r^{2}g^{2}K(g)} + \left(g'^{2} + \frac{a^{2}g^{2}}{r^{2}}\right)K(g)$$
$$+ V(g), \tag{36a}$$

$$T_{01} = -\frac{2K(g)eag^{2}A_{0}\sin\theta}{r}, \tag{36b}$$

$$T_{02} = \frac{2\mathscr{L}_{X}eag^{2}A_{0}\cos\theta}{r}, \tag{36c}$$

$$T_{12} = K(g)\left(g'^{2} - \frac{a^{2}g^{2}}{r^{2}}\right)\sin(2\theta), \tag{36d}$$

$$T_{11} = K(g)\left(e^{2}g^{2}A_{0}^{2} + g'^{2}\left(2\cos^{2}\theta - 1\right)\right.$$
$$\left. + \frac{a^{2}g^{2}}{r^{2}}\left(2\sin^{2}\theta - 1\right)\right) - V(g), \tag{36e}$$

$$T_{22} = K(g)\left(e^{2}g^{2}A_{0}^{2} + g'^{2}\left(2\sin^{2}\theta - 1\right)\right.$$
$$\left. + \frac{a^{2}g^{2}}{r^{2}}\left(2\cos^{2}\theta - 1\right)\right) - V(g). \tag{36f}$$

The equations of motion (35a), (35b), and (35c) are coupled differential equations of second order. To simplify the problem and get first-order equations, we follow [66] and take the stressless condition, $T_{ij} = 0$. This leads to

$$g' = \frac{ag}{r}$$
$$\text{and } e^{2}A_{0}^{2}g^{2}K(g) = V(g). \tag{37}$$

We can combine this with Gauss' law (35b) to get the two first-order equations
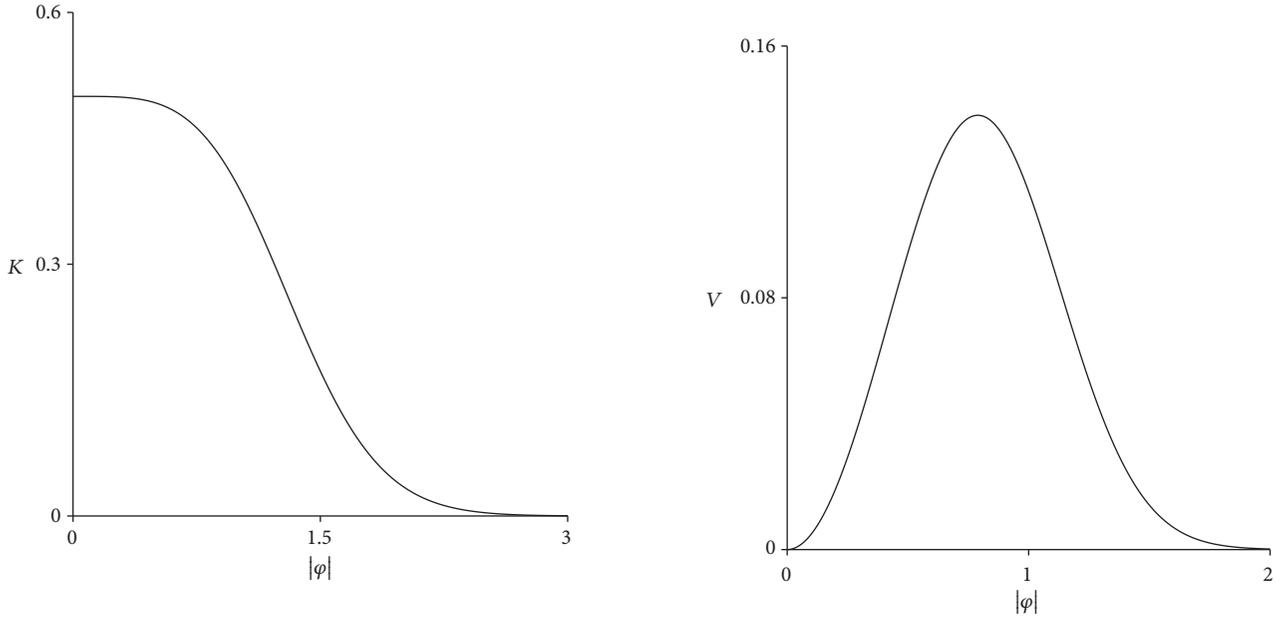
$$g' = \frac{ag}{r}$$
$$\text{and } \frac{a'}{r} = -\frac{2e^{2}g}{\kappa}\sqrt{KV}, \tag{38}$$

in which the functions $K(|\varphi|)$ and $V(|\varphi|)$ are constrained by

$$\frac{d}{dg}\left(\sqrt{\frac{V}{g^{2}K}}\right) = -\frac{2e^{2}}{\kappa}gK. \tag{39}$$

For $K(|\varphi|) = 1$ we have the potential given by $V(|\varphi|) = e^{4}|\varphi|^{2}(1-|\varphi|^{2})^{2}/\kappa^{2}$, which was studied in [27]. The first-order equations allow us to introduce an auxiliary function $W(a, g)$, given by

$$W(a, g) = -\frac{\kappa a}{e^{2}g}\sqrt{\frac{V(g)}{K(g)}}, \tag{40}$$

FIGURE 7: The function $K(|\varphi|)$ (left) and the potential $V(|\varphi|)$ (right) given by (43a) and (43b).

and write the energy density in (36a) as

$$\rho = \frac{1}{r}\frac{dW}{dr}. \tag{41}$$

By integrating it, we get the energy

$$E = 2\pi \left| W\left(a\left(\infty\right), g\left(\infty\right)\right) - W\left(a\left(0\right), g\left(0\right)\right)\right|$$
$$= 2\pi \left| W\left(0, v\right) - W\left(n, 0\right)\right|. \tag{42}$$

This formalism allows us to calculate the energy of the stressless solutions without knowing their explicit form. As done in the latter section, for simplicity, we neglect the parameters and work with unit vorticity, $n = 1$. Next, we present models in the above class that admit vortices in potentials with minima located at infinity, i.e., $v \longrightarrow \infty$ in the boundary conditions (6).

3.1. First Model. To start the investigation with the Chern-Simons dynamics, we consider the same $K(|\varphi|)$ of (17a) and (17b) but with other potential in order to satisfy the constraint (39). We then take

$$K\left(|\varphi|\right) = \frac{1}{2}\mathrm{sech}^2\left(\frac{1}{2}|\varphi|^2\right), \tag{43a}$$

$$V\left(|\varphi|\right)$$
$$= \frac{1}{2}|\varphi|^2\,\mathrm{sech}^2\left(\frac{1}{2}|\varphi|^2\right)\left(1 - \tanh\left(\frac{1}{2}|\varphi|^2\right)\right)^2. \tag{43b}$$

These functions are plotted in Figure 7. The potential presents a minimum at $|\varphi| = 0$ and a set of minima at $|\varphi| \longrightarrow \infty$. Its maximum is located at $|\varphi_m| \approx 0.79$, such that $V(|\varphi_m|) \approx 0.14$. Furthermore, even though the function $K(|\varphi|)$ is the same of (17a) and (17b) in Maxwell dynamics,

we see its corresponding potential has a completely different behavior near the origin in the Chern-Simons dynamics, with a minimum instead of a maximum at $|\varphi| = 0$.

The first-order equations (38) in this case read

$$g' = \frac{ag}{r}, \tag{44}$$

$$\frac{a'}{r} = -g^2\mathrm{sech}^2\left(\frac{g^2}{2}\right)\left(1 - \tanh\left(\frac{g^2}{2}\right)\right). \tag{45}$$

We have not been able to find analytical solutions for them. However, the behavior of the solutions near the origin may be studied by taking $a(r) = 1 - a_0(r)$ and $g(r) = g_0(r)$, similarly to the previous sections. By substituting them in the above equations, we get that

$$a_0\left(r\right) \propto r^4$$
$$\text{and } g_0\left(r\right) \propto r. \tag{46}$$

This helps as a guide in the numerical calculations. In Figure 8, we plot the solutions. In fact, we see the behavior of the functions near the origin as given above. These solutions behave similarly to the ones in Maxwell dynamics: $g(r)$ goes to infinity as r increases but $a(r)$ tends to zero very slowly, presenting a tail that goes far away from the origin. This feature is the opposite of the one found for compact Chern-Simons vortices in [69].

We now turn our attention to the auxiliar function $W(a, g)$ from (40). It is given by

$$W\left(a, g\right) = -a + a\tanh\left(\frac{g^2}{2}\right). \tag{47}$$

This is exactly the same function that appears in (20). By using (42), we get that the energy of the stressless solutions is
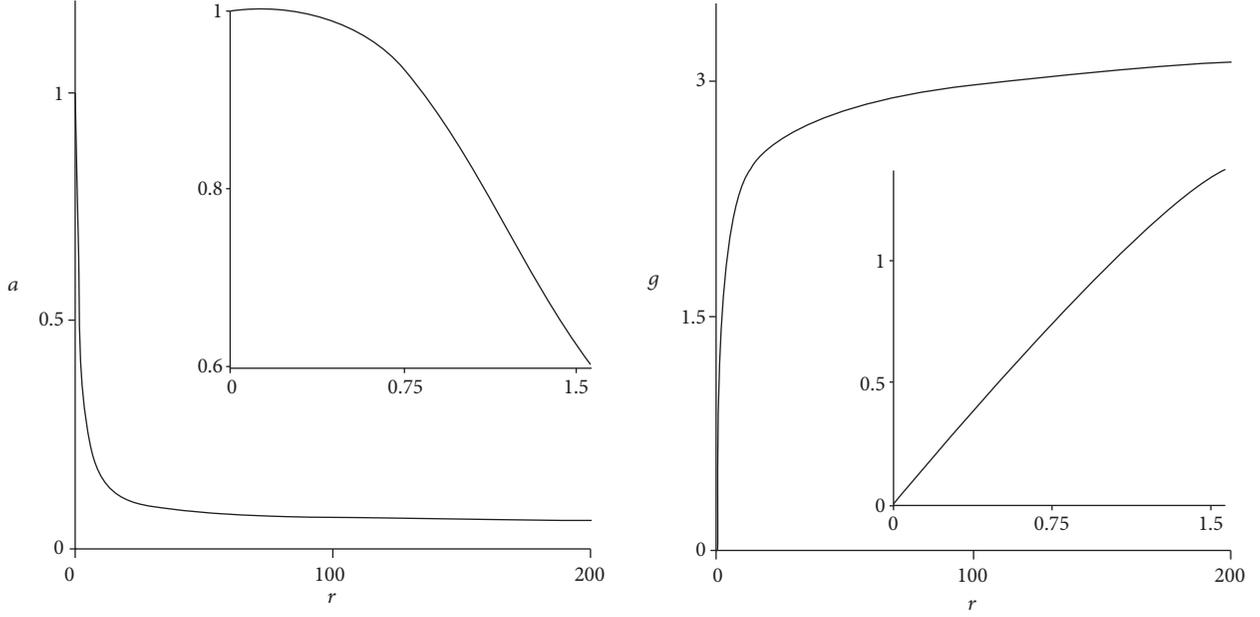
FIGURE 8: The functions $a(r)$ (left) and $g(r)$ (right), solutions of (44). The insets show the behavior near the origin, in the interval $r \in [0, 1.57]$.

$E = 2\pi$. To calculate the electric field intensity and the magnetic field, one has to use the numerical solutions of (44) in (32). The energy density must be calculated in a similar manner, by using the expression given below, which comes from (36a):

$$
\begin{aligned}
\rho = {} & \frac{a'^2}{2r^2 g^2} \cosh^2 \left(\frac{g^2}{2} \right) \\
& + \frac{1}{2} \left(g'^2 + \frac{a^2 g^2}{r^2} \right) \operatorname{sech}^2 \left(\frac{g^2}{2} \right) \\
& + \frac{1}{2} g^2 \operatorname{sech}^2 \left(\frac{g^2}{2} \right) \left(1 - \tanh \left(\frac{g^2}{2} \right) \right)^2 .
\end{aligned}
\tag{48}
$$

In Figure 9, we plot the electric field, the magnetic field, the temporal component of the gauge field from (33), and the energy density. As in the previous models, a numerical integration of the magnetic field and energy density gives the flux $\Phi \approx 2\pi$ and energy $\rho \approx 2\pi$. Thus, the tail of the solutions does not seem to contribute to change the topological charge, since it is given by the flux. Therefore, in the Chern-Simons scenario, vortices in vacuumless systems have the topological current (9) well defined that does not require any special definitions as done in [5] for kinks.

3.2. Second Model.

We now present a new model, given by the functions

$$
K (|\varphi|) = \frac{1}{2} \frac{\operatorname{sech}^2 (|\varphi|) \tanh^2 (|\varphi|)}{|\varphi|},
\tag{49a}
$$

$$
\begin{aligned}
& V (|\varphi|) \\
& = \frac{1}{18} |\varphi| \operatorname{sech}^2 (|\varphi|) \tanh^2 (|\varphi|) \left(1 - \tanh^3 (|\varphi|) \right)^2 .
\end{aligned}
\tag{49b}
$$

Differently of the previous model, the minima of both $K(|\varphi|)$ and the potential are located at $|\varphi| = 0$ and $|\varphi| \longrightarrow \infty$. The potential presents a maximum at $|\varphi_m| \approx 0.7500$, such that $V(|\varphi_m|) \approx 0.0055$. These features can be seen in Figure 10, in which we have plotted $K(|\varphi|)$ and the potential.

To calculate our solutions, we consider the first-order equations (38) to get

$$
g' = \frac{ag}{r},
\tag{50}
$$

$$
\frac{a'}{r} = -\frac{1}{3} g \operatorname{sech}^2 (g) \tanh^2 (g) \left(1 - \tanh^3 (g) \right).
\tag{51}
$$

We have not been able to find the analytical solutions of the above equations. Nevertheless, it is worth to estimate their behavior near the origin by taking $a(r) = 1 - a_0(r)$ and $g(r) = g_0(r)$, similarly to what was done before for the latter models. This approach leads to

$$
\begin{aligned}
& a_0 (r) \propto r^5 \\
& \text{and } g_0 (r) \propto r.
\end{aligned}
\tag{52}
$$

In Figure 11 we plot the solutions of (50). Notice that $a(r)$ is almost constant near the origin. This is due to the form of (52). As in the previous models, $g(r)$ tends to infinity as r becomes larger and larger. Also, we see $a(r)$ tends to vanish very slow when $r \longrightarrow \infty$, also presenting a tail which extends far away from the origin.

In this case, the function $W(a, g)$ in (40) becomes

$$
W (a, g) = \frac{a}{3} \left(1 - \tanh^3 (g) \right).
\tag{53}
$$

Therefore, by using (42), we conclude that the energy is $E = 2\pi/3$. To calculate the intensity of the electric and magnetic
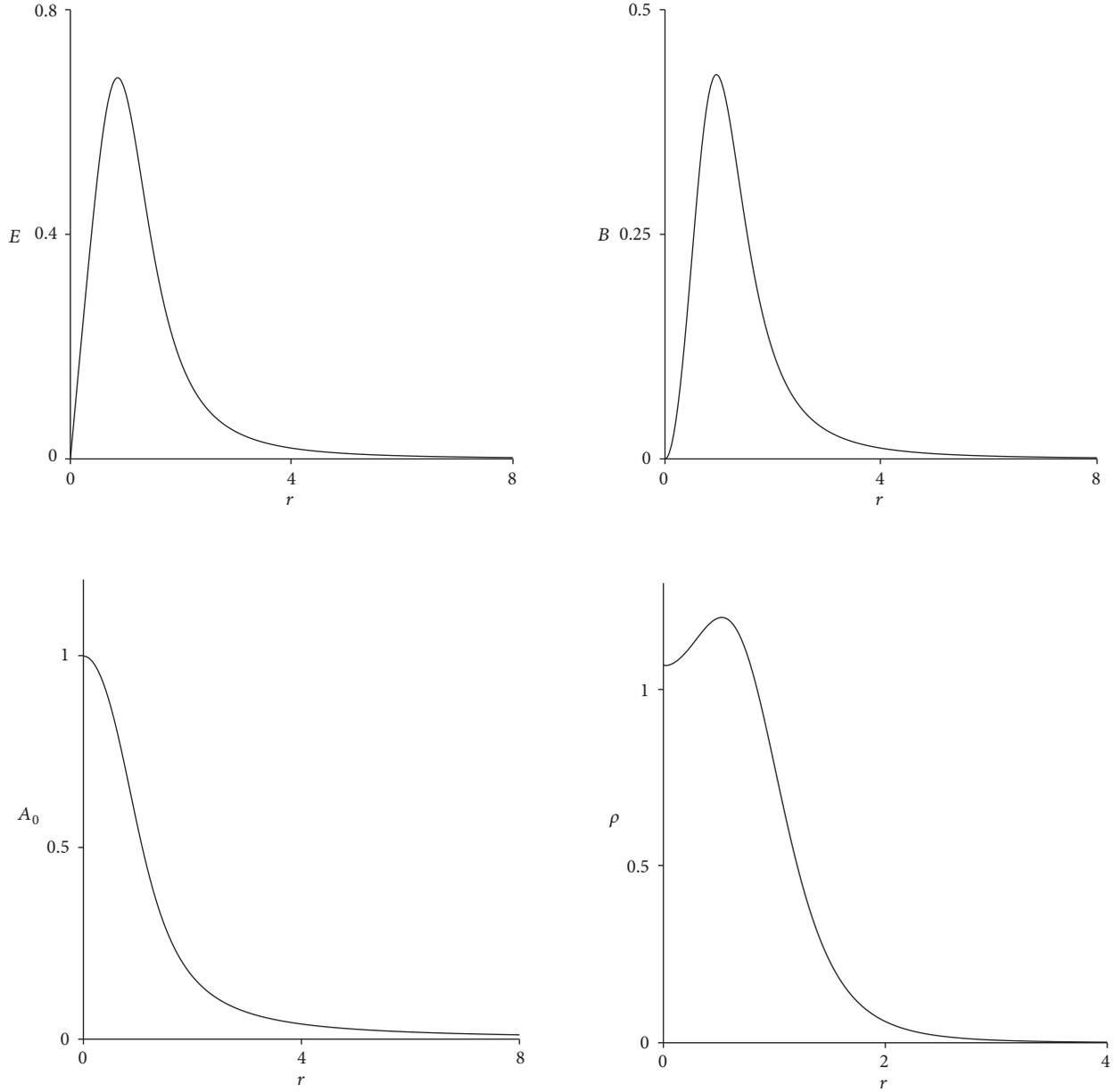
FIGURE 9: The electric field (upper left), the magnetic field (upper right), the temporal gauge field component (bottom left), and the energy density (bottom right) for the solutions of (44).

fields, one has to use the numerical solutions into (32). The same occurs to evaluate the energy density, which comes from (36a) that leads to

$$\rho = \frac{a'^2}{2r^2 g} \cosh^2(g) \coth^2(g)$$

$$+ \left(g'^2 + \frac{a^2 g^2}{r^2} \right) \frac{\operatorname{sech}^2(g) \tanh^2(g)}{2g} \qquad (54)$$

$$+ \frac{1}{18} g \operatorname{sech}^2(g) \tanh^2(g) \left(1 - \tanh^3(g) \right)^2.$$

In Figure 12, we plot the electric and magnetic fields, the temporal gauge component (33), and the above energy density. As for all of our previous models, the topological charge, given by the flux, remains unchanged from (8), having the value $\Phi \approx 2\pi$ obtained from a numerical integration. The energy can be obtained numerically and it is given by $E \approx 2\pi/3$, the same value obtained from the function $W(a, g)$ of (53). Also, we see the energy density in this model presents a valley deeper than in the previous one.

4. Conclusions

In this work, we have investigated vortices in vacuumless systems with Maxwell and Chern-Simons dynamics. In both scenarios, we have studied the properties of the generalized models in the classes (1) and (28) and, following [66], we
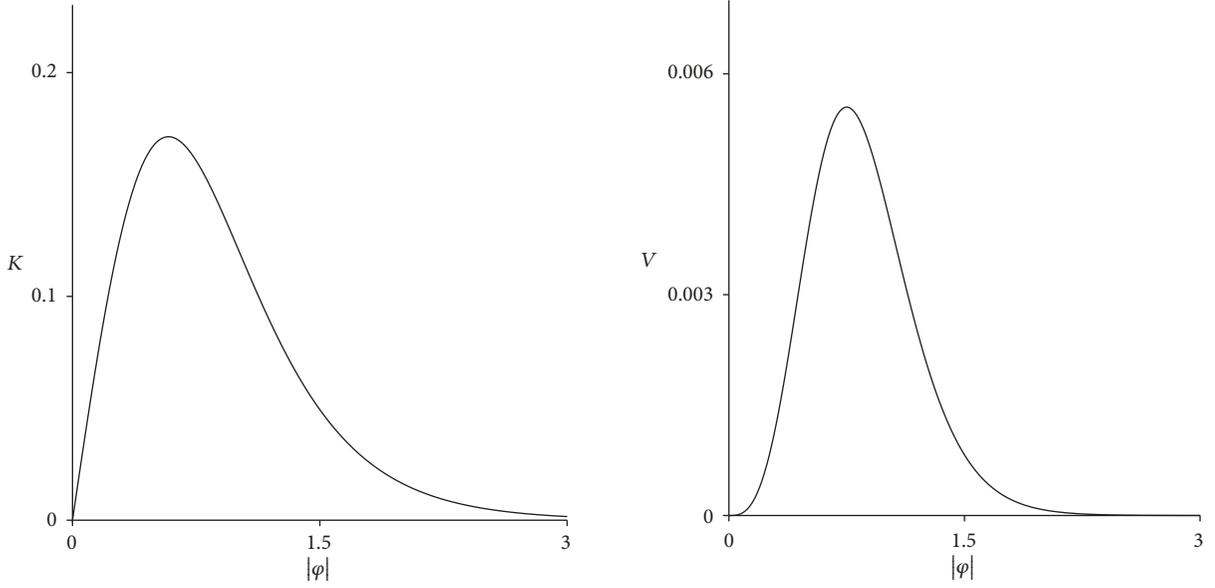
Figure 10: The function $K(|\varphi|)$ (left) and the potential $V(|\varphi|)$ (right) given by (49a) and (49b).
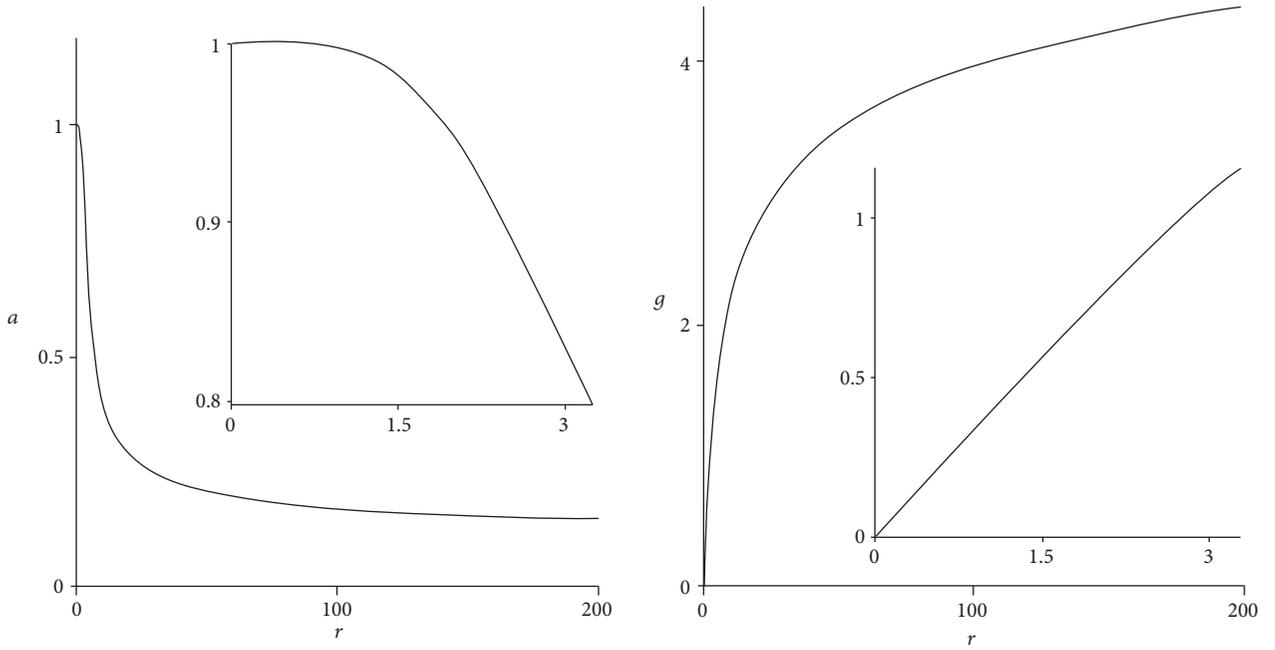

Figure 11: The functions $a(r)$ (left) and $g(r)$ (right), solutions of (50). The insets show the behavior near the origin, in the interval $r \in [0, 3.27]$.

have used a first-order formalism that allows calculating the energy without knowing the explicit form of the solutions.

The behaviors of the potentials are different at $|\varphi| = 0$, depending on the scenario; in the Maxwell case, they are nonvanishing, whilst in the Chern-Simons models they are zero. The hole around the origin in the potentials for the Chern-Simons dynamics makes the magnetic field vanish at $r = 0$. Regardless of the differences in the behavior of the magnetic field, the magnetic flux is always quantized by the vorticity n. Furthermore, even though we have worked only with $n = 1$,

for simplicity, in our examples, it is worth commenting that we have checked the energy is also quantized by the vorticity, n.

An interesting result is that the vortex solutions in vacuumless systems present a large tail that extends far away from the origin. The scalar field is asymptotically divergent and has infinite amplitude. Then, the solutions lose the locality. However the electric field, if it exists, the magnetic field, and the energy density are localized. This avoids the possibility of having infinite energies and fluxes. The flux is well defined and still works as a topological invariant. Unlike the kinks, we
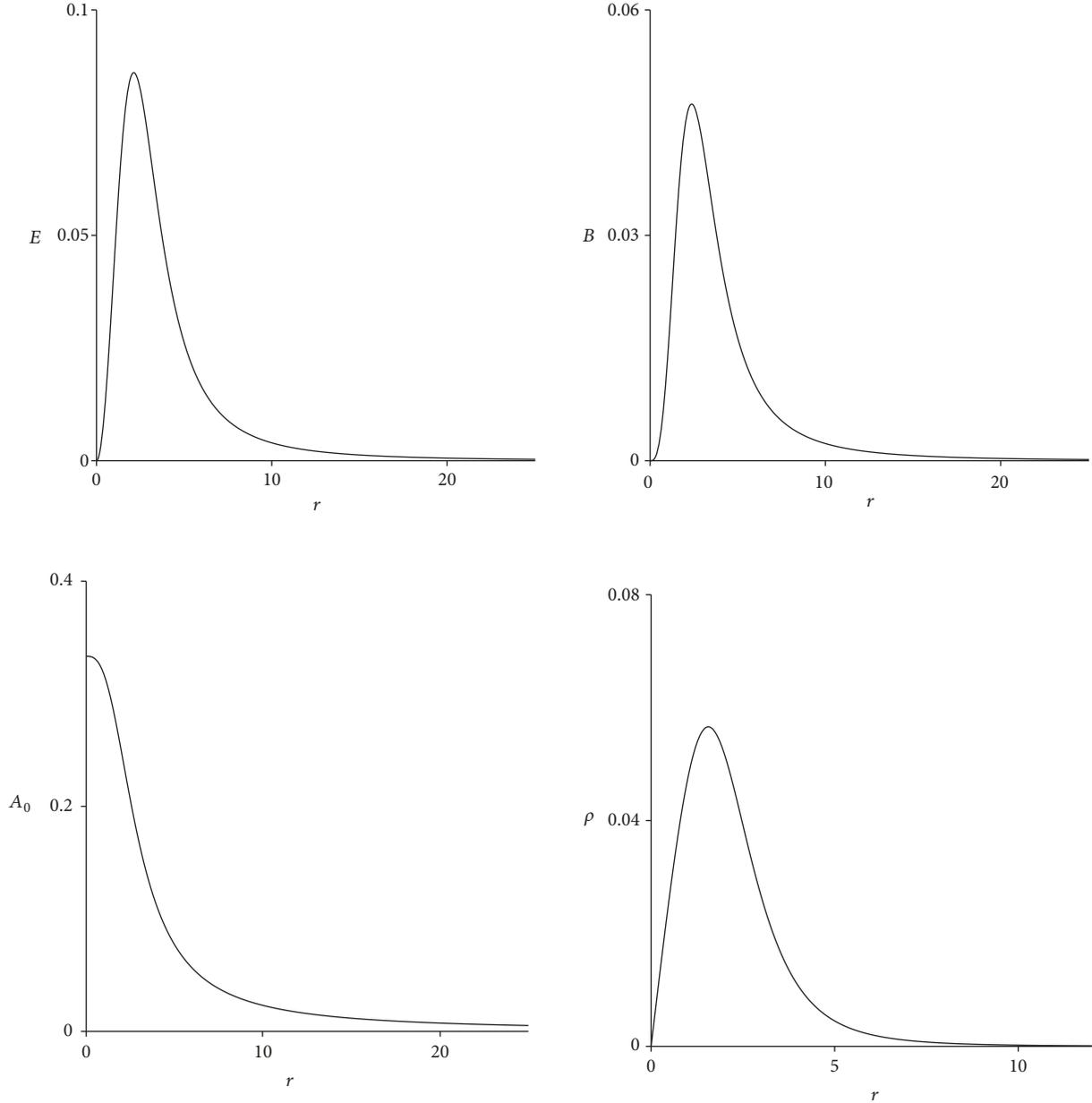
FIGURE 12: The electric field (upper left), the magnetic field (upper right), the temporal gauge component (bottom left), and the energy density (bottom right) for the solutions of (50).

concluded that vortices in vacuumless systems do not require any special definition of the topological current to study its topological character.

We then discovered vortices with a new behavior, whose solutions present a long tail. We hope these results encourage new research in the area, stimulating the study of new models in this and other contexts. One can follow the direction of [14] and study the demeanor of fermions in the background of these vortex structures. Also, the collective behavior of these vortices seems of interest, since it may give rise to non-standard interactions due to the particular aforementioned features of the solutions. Furthermore, following the lines of [6], one also can study the gravitational field of these

vortices. Another perspective is to investigate these structures in models with enlarged symmetries [35–38, 71–73], which may make them appear in the hidden sector, for instance. Finally, one may try to extend the current investigation to other topological structures, such as monopoles [74, 75], and nontopological structures, such as lumps [76–78] and Q-balls [70, 79]. Some of these issues are under consideration and will be reported in the near future.

Data Availability

The data used to support the findings of this study are included within the article.

Conflicts of Interest

Acknowledgments

References

[1] A. Vilenkin and E. P. Shellard, *Cosmic Strings and Other Topological Defects*, Cambridge Monographs on Mathematical Physics, Cambridge University Press, Cambridge, UK, 2007.

[2] N. Manton and P. Sutcliffe, *Topological Solitons*, Cambridge University Press, Cambridge, UK, 2007.

[3] T. Vachaspati, *Kinks and Domain Walls: An Introduction to Classical and Quantum Solitons*, Cambridge University Press, Cambridge, UK, 2007.

[4] I. Cho and A. Vilenkin, "Vacuum defects without a vacuum," *Physical Review D*, vol. 59, Article ID 021701, 1999.

[5] D. Bazeia, "Topological solitons in a vacuumless system," *Physical Review D*, vol. 60, Article ID 067705, 1999.

[6] I. Cho and A. Vilenkin, "Gravitational field of vacuumless defects," *Physical Review D*, vol. 59, Article ID 063510, 1999.

[7] D. Bazeia, F. A. Brito, and J. R. S. Nascimento, "Supergravity brane worlds and tachyon potentials," *Physical Review D*, vol. 68, Article ID 085007, 2003.

[8] A. de Souza Dutra and A. C. Amaro de Faria, "Vacuumless kink systems from vacuum systems: An example," *Physical Review D*, vol. 72, Article ID 087701, 2005.

[9] D. Bazeia, F. A. Brito, and L. Losano, "Scalar fields, bent branes, and RG flow," *Journal of High Energy Physics*, vol. 0611, p. 064, 2006.

[10] D. Bazeia, F. A. Brito, and F. G. Costa, "First-order framework and domain-wall/brane-cosmology correspondence," *Physics Letters B*, vol. 661, p. 179, 2008.

[11] G. P. de Brito and A. de Souza Dutra, "Multikink solutions and deformed defects," *Annals of Physics*, vol. 351, p. 620, 2014.

[12] F. C. Simas, A. R. Gomes, and K. Z. Nobrega, "Degenerate vacua to vacuumless model and kink-antikink collisions," *Physics Letters. B. Particle Physics, Nuclear Physics and Cosmology*, vol. 775, pp. 290–296, 2017.

[13] D. Bazeia and D. C. Moreira, "From sine-Gordon to vacuumless systems in flat and curved spacetimes," *The European Physical Journal C*, vol. 77, p. 884, 2017.

[14] D. Bazeia, A. Mohammadi, and D. C. Moreira, "Fermion bound states in geometrically deformed backgrounds," *Chinese Physics C*, vol. 43, Article ID 013101, 2019.

[15] A. M. Perelomov, *Integrable Systems of Classical Mechanics and Lie Algebras*, vol. I, Birkhäuser Basel, Basel, Switzerland, 1990.

[16] I. Affleck, M. Dine, and N. Seiberg, "Dynamical supersymmetry breaking in supersymmetric QCD," *Nuclear Physics B*, vol. 241, p. 493, 1984.

[17] P. J. E. Peebles and B. Ratra, "Cosmology with a time-variable cosmological 'constant'," *The Astrophysical Journal Letters*, vol. 325, p. L17, 1988.

[18] R. R. Caldwell, R. Dave, and P. J. Steinhardt, "Cosmological imprint of an energy component with general equation of state," *Physical Review Letters*, vol. 80, Article ID 1582, 1998.

[19] H. B. Nielsen and P. Olesen, "Vortex-line models for dual strings," *Nuclear Physics B*, vol. 61, pp. 45–61, 1973.

[20] H. J. de Vega and F. A. Schaposnik, "Classical vortex solution of the Abelian Higgs model," *Physical Review D: Particles, Fields, Gravitation and Cosmology*, vol. 14, no. 4, pp. 1100–1106, 1976.

[21] E. Bogomol'nyi, "The stability of classical solutions," *Soviet Journal of Nuclear Physics*, vol. 24, no. 4, pp. 449–454, 1976.

[22] M. Prasad and C. Sommerfield, "Exact classical solution for the 't hooft monopole and the julia-zee dyon," *Physical Review Letters*, vol. 35, p. 760, 1975.

[23] S.-S. Chern and J. Simons, "Characteristic forms and geometric invariants," *Annals of Mathematics*, vol. 99, p. 48, 1974.

[24] S. Deser, R. Jackiw, and S. Templeton, "Topologically massive gauge theories," *Annals of Physics*, vol. 140, no. 2, pp. 372–411, 1982.

[25] S. Deser, R. Jackiw, and S. Templeton, "Three-dimensional massive gauge theories," *Physical Review Letters*, vol. 48, p. 975, 1982.

[26] J. Hong, Y. Kim, and P. Y. Pac, "Multivortex solutions of the Abelian Chern-Simons-Higgs theory," *Physical Review Letters*, vol. 64, p. 2230, 1990.

[27] R. Jackiw and E. J. Weinberg, "Self-dual Chern-Simons vortices," *Physical Review Letters*, vol. 64, p. 2234, 1990.

[28] R. Jackiw, K. Lee, and E. J. Weinberg, "Self-dual Chern-Simons solitons," *Physical Review D*, vol. 42, p. 3488, 1990.

[29] G. Dunne, *Self-dual Chern-Simons Theories*, Springer-Verlag, 1995.

[30] E. Fradkin, *Field Theories of Condensed Matter Physics*, Cambridge University Press, 2013.

[31] A. J. Long, J. M. Hyde, and T. Vachaspati, "Cosmic strings in hidden sectors: 1. radiation of standard model particles," *Journal of Cosmology and Astroparticle Physics*, vol. 09, p. 030, 2014.

[32] A. J. Long and T. Vachaspati, "Cosmic strings in hidden sectors: 2. cosmological and astrophysical signatures," *Journal of Cosmology and Astroparticle Physics*, vol. 12, p. 040, 2014.

[33] A. E. Nelson and J. Scholtz, "Dark light, dark matter, and the misalignment mechanism," *Physical Review D*, vol. 84, Article ID 103501, 2011.

[34] P. Arias, D. Cadamuro, M. Goodsell et al., "WISPy cold dark matter," *Journal of Cosmology and Astroparticle Physics*, vol. 06, p. 013, 2012.

[35] P. Arias and F. A. Schaposnik, "Vortex solutions of an Abelian Higgs model with visible and hidden sectors," *Journal of High Energy Physics*, vol. 1412, p. 011, 2014.

[36] P. Arias, E. Ireson, C. Núñez, and F. Schaposnik, "N=2 SUSY Abelian Higgs model with hidden sector and BPS equations," *Journal of High Energy Physics*, vol. 1502, p. 156, 2015.

[37] D. Bazeia, L. Losano, M. A. Marques, and R. Menezes, "Vortices in a generalized Maxwell-Higgs model with visible and hidden sectors," https://arxiv.org/abs/1805.07369.

[38] D. Bazeia, M. A. Marques, and R. Menezes, "Maxwell-Higgs vortices with internal structure," *Physics Letters B*, vol. 780, p. 485, 2018.

[39] A. Hubert and R. Schäfer, *Magnetic Domains. The Analysis of Magnetic Microstructures*, Springer-Verlag, 1998.

[40] L. E. Sadler, J. M. Higbie, S. R. Leslie, M. Vengalattore, and D. M. Stamper-Kurn, "Spontaneous symmetry breaking in

a quenched ferromagnetic spinor Bose-Einstein condensate," *Nature*, vol. 443, p. 312, 2006.

[41] M. Vengalattore, S. R. Leslie, J. Guzman, and D. M. Stamper-Kurn, "Spontaneously modulated spin textures in a dipolar spinor bose-einstein condensate," *Physical Review Letters*, vol. 100, Article ID 170403, 2008.

[42] M. O. Borgh, J. Lovegrove, and J. Ruostekoski, "Internal structure and stability of vortices in a dipolar spinor bose-einstein condensate," *Physical Review A*, vol. 95, Article ID 053601, 2017.

[43] E. Babichev, "Global topological k-defects," *Physical Review D: Covering Particles, Fields, Gravitation, and Cosmology*, vol. 74, Article ID 085004, 2006.

[44] E. Babichev, "Gauge k-vortices," *Physical Review D: Covering Particles, Fields, Gravitation, and Cosmology*, vol. 77, Article ID 065021, 2008.

[45] J. Lee and S. Nam, "Bogomol'nyi equations of Chern-Simons Higgs theory from a generalized abelian Higgs model," *Physics Letters B*, vol. 261, no. 4, pp. 437–442, 1991.

[46] M. Neubert, "Symmetry-breaking corrections to meson decay constants in the heavy-quark effective theory," *Physical Review D: Particles, Fields, Gravitation and Cosmology*, vol. 46, p. 1879, 1992.

[47] C. Armendáriz-Picón, T. Damour, and V. Mukhanov, "k-Inflation," *Physics Letters B*, vol. 458, no. 2-3, pp. 209–218, 1999.

[48] C. Armendariz-Picon, V. Mukhanov, and P. J. Steinhard, "Dynamical solution to the problem of a small cosmological constant and late-time cosmic acceleration," *Physical Review Letters*, vol. 85, p. 4438, 2000.

[49] C. Armendariz-Picon, V. Mukhanov, and P. J. Steinbardt, "Essentials of k-essence," *Physical Review D: Particles, Fields, Gravitation and Cosmology*, vol. 63, Article ID 103510, 2001.

[50] X.-H. Jin, X.-Z. Li, and D.-J. Liu, "A gravitating global k-monopole," *Classical and Quantum Gravity*, vol. 24, no. 11, pp. 2773–2780, 2007.

[51] D. Bazeia, L. Losano, R. Menezes, and J. C. R. E. Oliveira, "Generalized global defect solutions," *The European Physical Journal C*, vol. 51, no. 4, pp. 953–962, 2007.

[52] S. Sarangi, "DBI global strings," *Journal of High Energy Physics*, vol. 018, p. 0807, 2008.

[53] D. Bazeia, L. Losano, and R. Menezes, "First-order framework and generalized global defect solutions," *Physics Letters B*, vol. 668, no. 3, pp. 246–252, 2008.

[54] C. Adam, P. Klimas, J. Sánchez-Guillén, and A. Wereszczyński, "Compact gauge K vortices," *Journal of Physics A: Mathematical and Theoretical*, vol. 42, Article ID 135401, 2009.

[55] D. Bazeia, A. R. Gomes, L. Losano, and R. Menezes, "Braneworld models of scalar fields with generalized dynamics," *Physics Letters B*, vol. 671, p. 402, 2009.

[56] D. Bazeia, E. da Hora, C. dos Santos, and R. Menezes, "BPS solutions to a generalized Maxwell–Higgs model," *The European Physical Journal C*, vol. 71, p. 1833, 2011.

[57] R. Casana, M. M. Ferreira Jr., and E. da Hora, "Generalized BPS magnetic monopoles," *Physical Review D: Covering Particles, Fields, Gravitation, and Cosmology*, vol. 86, Article ID 085034, 2012.

[58] R. Casana, E. da Hora, D. Rubiera-Garcia, and C. dos Santos, "Topological vortices in generalized Born–Infeld–Higgs electrodynamics," *The European Physical Journal C*, vol. 75, p. 380, 2015.

[59] H. S. Ramadhan, "Measurement of spin correlations in $t\bar{t}$ production using the matrix element method in the muon+jets final state in pp collisions at $\sqrt{s}$ = 8TeV," *Physics Letters B*, vol. 758, pp. 321–346, 2016.

[60] A. N. Atmaja, H. S. Ramadhan, and E. da Hora, "More on Bogomol'nyi equations of three-dimensional generalized Maxwell-Higgs model using on-shell method," *Journal of High Energy Physics*, vol. 1602, p. 117, 2016.

[61] R. Casana, A. Cavalcante, and E. da Hora, "Self-dual configurations in Abelian Higgs models with k-generalized gauge field dynamics," *Journal of High Energy Physics*, vol. 1612, p. 51, 2016.

[62] R. Casana, M. L. Dias, and E. da Hora, "Topological first-order vortices in a gauged $CP(2)$ model," *Physics Letters B*, vol. 768, pp. 254–259, 2017.

[63] D. Bazeia, M. A. Marques, and R. Menezes, "Generalized born-infeld–like models for kinks and branes," *EPL (Europhysics Letters)*, vol. 118, p. 11001, 2017.

[64] D. Bazeia, E. da Hora, C. dos Santos, and R. Menezes, "Generalized self-dual Chern-Simons vortices," *Physical Review D: Particles, Fields, Gravitation and Cosmology*, vol. 81, Article ID 125014, 2010.

[65] A. N. Atmaja, "A method for BPS equations of vortices," *Physics Letters B*, vol. 768, pp. 351–358, 2017.

[66] D. Bazeia, L. Losano, M. A. Marques, R. Menezes, and I. Zafalan, "First order formalism for generalized vortices," *Nuclear Physics B*, vol. 934, pp. 212–239, 2018.

[67] P. Rosenau and J. M. Hyman, "Compactons: Solitons with finite wavelength," *Physical Review Letters*, vol. 70, p. 564, 1993.

[68] D. Bazeia, L. Losano, M. A. Marques, R. Menezes, and I. Zafalan, "Compact vortices," *The European Physical Journal C*, vol. 77, p. 63, 2017.

[69] D. Bazeia, L. Losano, M. A. Marques, and R. Menezes, "Compact chern-simons vortices," *Physics Letters. B. Particle Physics, Nuclear Physics and Cosmology*, vol. 772, pp. 253–257, 2017.

[70] D. Bazeia, M. A. Marques, and R. Menezes, "Twinlike models for kinks, vortices, and monopoles," *Physical Review D: Particles, Fields, Gravitation and Cosmology*, vol. 96, no. 2, Article ID 025010, 2017.

[71] M. Shifman, "Simple models with non-Abelian moduli on topological defects," *Physical Review D*, vol. 87, Article ID 025025, 2013.

[72] A. Peterson, M. Shifman, and G. Tallarita, "Low energy dynamics of $U(1)$ vortices in systems with cholesteric vacuum structure," *Annals of Physics*, vol. 353, p. 48, 2014.

[73] A. Peterson, M. Shifman, and G. Tallarita, "Spin vortices in the Abelian–Higgs model with cholesteric vacuum structure," *Annals of Physics*, vol. 363, p. 515, 2015.

[74] G. 't Hooft, "Magnetic monopoles in unified gauge theories," *Nuclear Physics B*, vol. 79, no. 2, pp. 276–284, 1974.

[75] D. Bazeia, M. A. Marques, and R. Menezes, "Magnetic monopoles with internal structure," *Physical Review D: Covering Particles, Fields, Gravitation, And Cosmology*, vol. 97, Article ID 105024, 2018.

[76] A. T. Avelar, D. Bazeia, L. Losano, and R. Menezes, "New lump-like structures in scalar-field models," *The European Physical Journal C*, vol. 55, no. 1, pp. 133–143, 2008.

[77] A. T. Avelar, D. Bazeia, W. B. Cardoso, and L. Losano, "Lump-like structures in scalar-field models in 1+1 dimensions," *Physics Letters A*, vol. 374, pp. 222–227, 2009.

[78] D. Bazeia, M. A. Marques, and R. Menezes, "Compact lumps," *Physical Review D: Particles, Fields, Gravitation and Cosmology*, vol. 111, no. 6, p. 61002, 2015.

[79] S. R. Coleman, "Q-balls," *Nuclear Physics B*, vol. 262, pp. 263–283, 1985.